Generation and expansion of transitional lung organoids from human pluripotent stem cells.

Ivana Matkovic Leko,[1,2,6] Nadine Schrode,[3,4,6] Juan Torres,[1,2] Mikael Pezet,[1,2] Tania A. Thimraj,[1,2] Kristin G. Beaumont,[3,4,6] Hans-Willem Snoeck [1,2,5,6]

[1]Columbia Center for Human Development/Center for Stem Cell Therapies, Columbia University Irving Medical Center, New York, NY, USA

[2]Department of Medicine, Columbia University Irving Medical Center, New York, NY, USA

[3]Department of Genetic and Genomic Sciences, Icahn School of Medicine at Mount Sinai, New York, USA

[4]The Center for Advanced Genomic Technology, Icahn School of Medicine at Mount Sinai, New York, USA

[5]Department of Microbiology and Immunology, Columbia University Irving Medical Center, New York, NY, USA

[6]These authors contributed equally

Corresponding authors/contacts

Hans-Willem Snoeck, MD, PhD
Byron M Thomashow Professor of Medicine
Director, Center for Stem Cell Therapies
Division of Pulmonary Medicine, Allergy and Critical Care
Departments of Medicine, and Microbiology & Immunology
Columbia University Vagelos College of Physicians and Surgeons
650 W. 168th Street, BB 801E
New York, NY 10032
(T) 212 342 0182
(F) 212 342 0550
hs2680@columbia.edu

Kristin G. Beaumont, PhD
Assistant Professor
Associate Director, Center for Advanced Genomic Technology
Department of Genetics and Genomic Sciences
Icahn School of Medicine at Mount Sinai
1425 Madison Ave.
New York, NY 10029
(T) 212 659 8317
kristin.beaumont@mssm.edu

Several novel distal lung populations were recently identified that may be involved in regeneration after injury.[1–3] As these are absent in rodents, a deeper understanding of their roles and lineage relations requires availability of equivalent cells *in vitro*. Here we report the generation of expandable, clonal spheres, called 'transitional lung organoids' (TLOs), from human pluripotent stem cells. TLOs consist mainly of previously identified type 0 alveolar epithelial (AT0) cells, terminal respiratory bronchiole stem cells and distal basal cells (BCs).[3] Velocity analysis of single cell RNAseq data suggests that distal BCs are the most undifferentiated progenitors in the TLOs and give rise to AT0 cells. TLOs will be an important resource for studies in human lung regeneration, and potentially for regenerative approaches for human lung disease.

The respiratory epithelium contains basal (BC), ciliated, secretory, goblet and neuroendocrine cells in the airways, and alveolar type 1 (AT1) and surfactant-producing alveolar type 2 (AT2) cells in the alveoli, where gas exchange takes place.[4,5] Additional complexity was discovered when transitional populations were identified in the terminal bronchioles (also called respiratory airways) of primates and ferrets, but not rodents, that may play a role in regeneration, as they were more abundant after lung injury.[1–3] A feature of at least some of these populations is the expression of the secretory cell marker, *SCGB3A2*, first reported by Haberman et al. who found *SCGB3A2*$^+$ cells co-expressing AT1 and AT2 markers in the distal lung.[1] Basil et al. also reported *SCGB3A2*$^+$ cells negative for the AT2 marker, *SFPTC*, in respiratory airways.[2] Murthy et al. identified multiple subpopulations characterized by co-expression of another AT2 marker, *SFTPB*.[3] These included *SCGB3A2*$^+$*SFTPB*$^+$*SFTPC*$^+$ 'AT0' cells, *SFTPB*$^+$S*CGB3A2*$^+$*SFTPC*$^-$ terminal respiratory bronchiole secretory cells (TRB-SCs), *SFTPB*$^+$S*CGB3A2*$^+$*SCGB1A1*$^+$ pre-TRB-SCs, and *SFPTB*$^+$*SCGB3A2*$^-$ distal BCs, some of which are low to negative for the airway BC markers, *KRT5* and *p63*. Based on airway organoids derived from human pluripotent stem cells (hPSCs), Basil et al.[2] proposed unidirectional differentiation of *SCGB3A2*$^+$ cells into AT2

cells, which was consistent with their Slingshot[6] pseudotime analysis. On the other hand, Murthy et al.,[3] using adult distal lung organoids, suggested that AT0 cells are transitional between AT2 and AT1 fates and can also give rise to TRB-SCs, a conclusion supporting their own Velocity trajectory analysis.[7] As currently available organoid models yielded conflicting data and as these cell types are not present in mice,[2,3] an *in vitro* model that contains a large fraction of these cells would complement *ex vivo* studies. Here we report the generation from hPSCs of expandable, clonal spheres containing these distal progenitor populations.

The GSK3 inhibitor CHIR, keratinocyte growth factor (KGF), dexamethasone, 3′,5′-cyclic adenosine monophosphate (cAMP), and 3-isobutyl-1-methylxanthine (IBMX) (CK-DCI) promote outgrowth of spheres containing AT2 cells (alveolospheres) from hPSC-derived lung progenitors enriched by sequential cell sorting for reporter genes or cell surface markers.[8–10] We previously reported the generation of fetal stage, branching distal lung organoids from hPSCs.[11] After dissociation of ESC or iPSC-derived organoids and culture as single cells in Matrigel with CK-DCI **(Fig. S1a)**, hollow spheres developed within 2 weeks **(Fig. 1a, Fig. S1a)**, which we call 'transitional lung organoids' (TLOs). TLOs were clonal as mixing single cells from organoids expressing GFP or mScarlet yielded only spheres expressing either fluorescent reporter **(Fig.S1b)**. TLOs highly expressed mRNAs encoding the AT2 markers, *SFTPC*, *SFTPB*, *ABCA3*, *LPCAT*, *NAPSA, SLC234A2*, and *LAMP3* **(Fig. 1b, Fig S1c)**. At variance with previously reported alveolospheres,[8,9] however, strong induction of *SCGB3A2* mRNA was observed **(Fig. 1b, Fig. S1c)**. Confocal microscopy revealed uniform expression of EPCAM, NKX2.1 and SFTPB with a subset of cells in each TLO also expressing pro-SFTPC and SCGB3A2 **(Fig. 1c, Fig. S1d,e)**. In some TLOs the presumably more mature AT2 marker, HT2-280,[12] **(Fig. 1c)**, was detected, which was confirmed by flow cytometry (3-25%, n = 4 ESC-derived and n = 1 iPSC-derived TLOs) **(Fig. 1d)**). Western Blot showed presence of fully processed SFTPC and SFTPB **(Fig 1f, Fig. S2a)**. Transmission electron microscopy revealed apical presence of lamellar bodies (LBs), a feature of

AT2 cells,[13] **(Fig 1g, Fig. S2b)**, consistent with the SFTPB staining pattern **(Fig. 1c)**. However, these had low electron density and where often organized as multivesicular bodies **(Fig. 1g, arrows),** while the cytoplasm contained glycogen **(Fig. 1g, stars)**, indicative of immaturity.[14,15] Consistent with abundant presence of LBs, TLOs showed apical accumulation of the lysosomal dye, LysoTracker Red**(Fig. S2c)**.

TLOs can be serially passaged every ~3 weeks for up to at least 7 passages with an average expansion of ~10-fold between each passage. Over this time, TLOs were phenotypically stable (**Fig. 1b** pooled from 9 lines derived from organoids at days 40, 60 and 120 and between one and six passages). Furthermore, they can be cryopreserved and thawed while retaining their expression profile **(Fig. S3a).**

As removing WNT signaling has been reported to induce AT2 maturation in alveolospheres,[9,10] we withdrew CHIR. CHIR withdrawal, however, led to disintegration **(Fig. S3b)**, proliferation arrest **(Fig. S3c)**, apoptosis **(Fig. S3d)** and loss of AT2 markers **(Fig. S3e)**, indicating that GSK3 inhibition is required for TLO maintenance and propagation. Despite similar culture conditions, TLOs therefore differ from previously reported alveolospheres,[9,10] which, in contrast to TLOs, do not contain SCGB3A2$^+$ cells,[2] undergo AT2 maturation after intermittent CHIR withdrawal,[9,10] and require reporter lines or enrichment steps for their generation.[8–10,16]

scRNAseq confirmed that almost all cells expressed *SFTPB*, *NKX2.1* and *EPCAM* and identified a distinct, large population of *SCGB3A2*$^+$ cells that expressed the most *SFTPB*. **(Fig. 2a)**. Markers of mature airway cells were absent, and, in contrast to previously reported alveolospheres,[9,10] contamination with gastric or intestinal cells was not detected (not shown). Clustering revealed 4 closely related clusters (0-3), and 3 small but more distinct clusters that each made up ~1% of the cells (4-6) **(Fig. 2b,** heatmap in **Fig. S4).** Cluster 0 contained cells expressing AT2 markers (*SFTPC*, *ABCA3, NAPSA*) and the highest levels of *SFTPB,* while clusters 0, 2 and 3 expressed *SCGB3A2* **(Fig. 2a)**. Cluster 1, at the other extreme, expressed

less *SFTPB* but did not express *SCGB3A2* or AT2 markers **(Fig. 2a)**. Cell type annotation using machine learning trained on the data of Murthy et al.[3] matched cluster 0 with AT0 cells (*SFTPB*$^+$*SCGB3A2*$^+$*SFTPC*$^+$*)* and TRB-SCs (*SFTPB*$^+$*SCGB3A2*$^+$*SFTPC*$^-$*)*. Cluster 1 corresponded to *SFTPB*$^+$*KRT5*$^-$*P63*$^-$*SCGB3A2*$^-$ distal BCs, primarily characterized by elevated expression of *IGFBP2* **(Fig. 2a, Fig. S4)**, a marker of airway and in particular of basal cells according to LungMap.[17] Clusters 2 and 3 were classified as a mixture of 'differentiating BCs' and rare 'immature AT1 cells', both likely representing differentiation intermediates **(Fig. 2c)**. No matches with any other populations were found. Trajectory analysis using scVelo[7] confirmed the notion that clusters 2 and 3 were intermediate between clusters 0 and 1, and showed differentiation pathways originating from distal BCs (cluster 1) and terminating in AT0 cells in cluster 0 **(Fig. 2c)**. Given the clonal nature of the TLOs, these findings suggest a lineage from distal BCs over TRB-SCs to AT0 cells that was not recognized in recent scRNAseq studies of human lung.[1–3,17,18] Cluster 4 are rare *ASCL1*$^+$ neuroendocrine cells, some of which, quite unusually, also expressed *SFTPB* and *SCGB3A2* **(Fig. 2a)** and may represent precursors. The small cluster 5 contained proliferating cells that could not be further identified, while the equally small cluster 6 is distinguished by four lncRNAs **(Fig. S4)**, and may also be a regenerative population.

Cell identity assignment based on the data of Haberman et al.,[1] also showed *SCGB3A2*$^+$ cells and transitional *SCGB3A2*$^+$ AT2 cells mainly in cluster 0, and classified the remainder as BCs (they did not describe specific BC subsets) and some rare SCGB3A2$^+$*SCGB1A1*$^+$ cells (likely closely related to pre-TRB-SCs from Murthy et al.[3]) **(Fig. 2e)**. Both training sets for cell identity assignment thus yielded consistent results.

The TLOs described here consist of a spectrum of recently identified potential distal lung progenitor cells.[1–3] Their clonality and scVelo analysis indicate close lineal hierarchy among the various cell types, with distal BCs probably the main progenitor population, at least in this *in vitro*

model. As these populations are absent in rodent models, TLOs will be an important resource to gain deeper insight into mechanism involved in normal and abnormal human lung regeneration, and may have applications in regenerative approaches for lung diseases.

Acknowledgments:

This work was supported by grants NIH HL120046 (HWS), NIH 1U01HL134760 (HWS), and NIH S10 OD032447 (HWS). This research was also funded by in part through the NIH/NCI Cancer Center Support Grant P30CA013696 and used the Tissue bank part of the Molecular Pathology Shared Resource.

Author Contributions

IML developed the generation of TLOs and performed most of the experiments, NS performed scRNAseq analysis, to which TAT contributed as well. KGB supervised scRNAseq work and analysis, JT performed Western Blots. MP provided critical conceptual input and hypothesized and showed that TLOs contain ATO cells. HWS provide concept, supervised and wrote the manuscript.

Competing interests

HWS and IML have file a provisional patent application on the generation of TLOs. The other authors declare no competing interests.

Methods

Human lung samples.

De-identified normal human lung samples were provided by the Herbert Irving Comprehensive Cancer Center Molecular Pathology Shared Resource Tissue Bank core under IRB-AAAT8682.

Maintenance of hPSCs

Before differentiation, Rockefeller University Embryonic Stem Cell Line 2 (RUES2, passage 24-32) or mRNAi PSC lines (generated using mRNA transfection and obtained from the Mount Sinai Stem Cell Core, NY) were maintained on mouse embryonic fibroblasts (MEFs) plated at 22,500 cells/cm^2. Cells were cultured in hESC maintenance media (DMEM/F12 (ThermoFisher, Carlsbad, CA), 20% Knock-out serum, (Stem Cell Technologies, Vancouver, BC), 0.1 mM β-mercaptoethanol (Sigma-Aldrich,Burlington, MA) , 0.2% Primocin (InvivoGen, San Diego, CA), 20 ng/ml FGF2 (R&D Systems/Biotechne, Minneapolis, MN), and 1% Glutamax (ThermoFisher)) which was changed daily. hPSCs were passaged every 3-4 days with Accutase (Innovative Cell Technologies, San Diego, CA) at least two times before differentiation, washed and replated at a dilution of 1:24. Cultures were maintained in a humidified 5% CO_2 atmosphere at 37°C. Lines are karyotyped and verified for Mycoplasma contamination using PCR (InVivoGen) every 6 months.

Generation of hESC-derived lung organoids

The hESC-derived human lung organoids were generated as described previously.[11] Briefly, MEFs were depleted by passaging 5-7x10^6 hESCs onto Matrigel (Corning, Corning, NY) coated 10-cm dish. Cells were maintained in hESC media in a humidified 5% CO_2 atmosphere at 37°C. After 24 hours, cells were detached with 0.05% Trypsin/EDTA (ThermoFisher) and distributed to the 6-well low attachment plate containing primitive streak/embryoid body media (10 μM Y-27632 (Tocris/Biotehne, Minneapolis, MN), 3 ng/ml BMP4 (R&D/Biotechne) to allow embryoid body

formation. Embryoid bodies were fed every day with fresh endoderm induction media (10 μM Y-27632, 0.5 ng/ml BMP4, 2.5 ng/ml FGF2 and 100 ng/ml ActivinA (R&D/Biotechne)) and maintained in a humidified 5% CO_2/5% O_2 atmosphere at 37°C. Endoderm yield efficiency was determined by dissociating embryoid bodies and evaluating CXCR4 and c-KIT (Biolegend, San Diego, CA) co-expression by flow cytometry on day 4. Cells used in all experiments had > 90% endoderm yield and were plated on 0.2% fibronectin-coated wells (R&D/Biotechne) at a density of 80,000 cells/cm^2. Cells were incubated in Anteriorization media-1 (100 ng/ml Noggin (R&D/Biotechne) and 10 μM SB431542 (Tocris)) for 24 hours, followed by Anteriorization media-2 (10 μM SB431542 (Tocris) and 1 μM IWP2 (Tocris)) for another 24 hours. At the end of anterior foregut endoderm induction, cells were switched to Ventralization/Branching media (3μM CHIR99021 (Tocris), 10 ng/ml FGF10 (R&D/Biotechne), 10 ng/ml rhKGF, (R&D/Biotechne), 10 ng/ml BMP4 and 50 nM *all-trans* Retinoic acid (Tocris)) for 48 hours and three-dimensional clump formation was observed. The adherent clumps were detached by gentle pipetting and transferred to the low-attachment plate, where they folded into lung bud organoids as early as d10-d12 (LBOs). Branching media was changed every other day until d20–d25 and LBOs were embedded in 100% Matrigel in 24-well transwell (BDFalcon, Franklin Lakes, NJ) inserts. Branching media was added after Matrigel solidified and changed every 2-3 days to facilitate proper growth into lung organoids. Culture of embedded organoids can be kept for more than 6 months.

Generation of transitional lung organoids (TLOs)

Matrigel embedded lung organoids can be used for TLO generation when they reach d42 of development. Media was removed from the transwell and 1 ml of 2 mg/ml dispase (Corning) was added to release lung organoid from the Matrigel for 30-45 minutes in normoxic incubator. The organoid was transferred to a 15 ml conical tube and washed with stop media (DMEM (Corning), 5% FBS (Atlanta Biologicals; Flowery Branch, Georgia), 1% Glutamax (ThermoFisher)) to neutralize Dispase, then centrifuged at 200 g for 5 minutes. The pellet was incubated with 1 ml of

0.05% Trypsin/EDTA in normoxic incubator for 10-12 minutes with occasional pipetting with a P1000 pipet tip. Single cell dissociation was verified using a bright field microscope. If a single cell suspension was not obtained after 12 minutes, cells were washed with stop media and incubated for additional 5 minutes with 0.05% Trypsin/EDTA. Cells were counted using a hemocytometer and 400 cells/μl of undiluted Matrigel were plated in a well of a 12-well non-tissue culture plate. The plate was placed in normoxic incubator for 30 minutes until Matrigel polymerized and 1 ml of CKDCI (3μM CHIR 99021, 10 ng/ml rhKGF, 50 ng/ml dexamethasone (ThermoFisher), 0.1 mM 8-Bromoadenosine 3′,5′-cyclic monophosphate sodium salt (Tocris) and 0.1 mM 3-Isobutyl-1-methylxanthine (Sigma-Aldrich)) media was gently added using 10 ml serological pipette. Media was changed every 3 days. After 2-3 weeks, a TLO culture is established at that can be maintained by regular passaging for more than six months.

RT-qPCR.

Total RNA was extracted according to manufacturer's instructions using the Direct-zol™ RNA Microprep (Zymo Research, Irvine, CA), and 500 ng of total RNA was reverse transcribed using the qScript™ XLT cDNA SuperMix (Quantabio, Beverly, MA). Technical triplicates of 15 ml reaction (for use in Applied Biosystems QuantStudio7 384-well System, Waltham, MA) were prepared with 3 ul of diluted cDNA and run for 40 cycles. Primers used are listed in **Table S1**. Relative gene expression was calculated based on the average cycle (Ct) value, normalized to *GAPDH* as the internal control and reported as fold change (2(-ddCT)).

Immunofluorescence.

After removal of media, a flat edge was used to carefully detach the Matrigel droplet with embedded TLOs from the bottom of the 12 well plate. The droplet was then transferred to an OCT histology mold and embedded in Tissue-Tek OCT Compound (Sakura Finetek, Torrance, CA). Frozen samples were cut on cryotome at the thickness of 10-12 mm and collected on adhesion

microscope slides, air-dried and fixed in 4% paraformaldehyde, then washed 2 times for 5 minutes in 50 mM glycine to inactivate PFA, followed by washing in PBS. Samples were permeabilized for 10 minutes in 0.2% PBST (PBS + 0.2% Triton X-100) and blocked by incubating in PBS containing 5% donkey serum, then incubated overnight in primary antibody **(Table S2)** in 0.2% Triton X-100 and 2% donkey serum. Next day, samples were washed three times in PBS and 1% donkey serum and incubated with secondary antibody (1:200, **Table S2**) for 1 hour at the room temperature. Nuclei were stained with DAPI (ThermoFisher) and sections were mounted with Mounting Reagent (DAKO, Santa Clara, CA) and coverslipped. Samples were imaged using a Leica TCS SP8 Stellaris Laser scanning confocal microscope, and Leica DMi1 Inverted Phase Contrast Microscope (Leica Microsystems, Deerfield, IL).

Flow cytometry

Spheres embedded in Matrigel were released by incubating with Dispase for 30-60 minutes, then washed and dissociated into single cells with 0.05% Trypsin/EDTA in normoxic incubator for 10-12 minutes with occasional pipetting with P1000. The single cell suspension was stained in polystyrene round-bottom 12 x 75 mm tubes (BD Falcon). Primary HTII-280 antibody (Terrace Biotech, San Francisco, CA, 1:150 dilution) was added to 150 µl of cell suspension and incubated for 1 hour at the room temperature. Cells were washed two times with FACS buffer (PBS, 10% FBS and 1% sodium azide) and centrifuged for 5 minutes at 1400 rpm. Fluorochrome-labeled secondary antibody (Alexa Fluor 488 goat anti-mouse IgM) in diluted in FACS buffer at 1:100 ratio was added for 30 minutes in the dark. Cells are washed two times by centrifugation. Conjugated human EPCAM antibody (Biolegend) was added for 30 minutes. Cells were washed and resuspended in FACS buffer for flow cytometric analysis.

Transmission Electron Microscopy

Transmission Electron Microscopy (TEM) was performed at the NYU Langone Medical Center Microscopy Core. TLOs were fixed with 2% paraformaldehyde and 2.5% glutaraldehyde in 0.1M sodium cacodylate buffer (pH7.2) for 2 hours and post-fixed with 1% osmium tetroxide for 1.5 hours at room temperature, then processed in a standard manner and embedded in EMbed 812 (Electron Microscopy Sciences, Hatfield, PA). Semi-thin sections were cut at 1 mm and stained with 1% Toluidine Blue to evaluate the quality of preservation and find the area of interest. Ultrathin sections (60 nm) were cut, mounted on copper grids and stained with uranyl acetate and lead citrate by standard methods. Stained grids were examined under Philips CM-12 electron microscope and photographed with a Gatan (4k ×2.7k) digital camera (Gatan, Inc., Pleasanton, CA).

Western Blot

Cultured cells embedded in Matrigel were released by incubating with Dispase (Corning) for 30 minutes. Cells were then washed, collected in PBS, and treated with lysis buffer (RIPA buffer, 1x Roche Complete Protease inhibitor cocktail, and Roche PhosSTOP). Buffer-treated cells were mechanically lysed using a 25-gauge needle and left on ice for 30 minutes. Human lung samples were homogenized with stainless steel beads and left to lyse on ice in lysis buffer for 4-6 hours. Samples were then centrifuged at 15,000 g for 10 minutes and the supernatant was collected and stored at -80°C until analysis. Protein concentration was measured using Pierce BCA Protein Assay Kit (ThermoFisher). A total of 18 µg of TLO, hPSC, and human lung lysate were loaded for mature SPC analysis and a total of 5 µg of each were loaded for mature SPB analysis. Lysates were resolved on pre-cast NuPage 4-12% Bis-Tris gels (Invitrogen) and transferred to nitrocellulose membranes (Bio-Rad, Hercules, CA). The following primary antibodies were used to probe the blots: mature SPC (1:1000, Seven Hills Bioreagents, Cincinatti, OH), mature SPB (1:1000, Seven Hills Bioreagents), GAPDH (1:5000, Cell Signaling Technology). Species-specific secondary antibodies with HRP conjugates (Cell Signaling Technology, Danvers, MA) were used

at 1:15,000 dilution. Blots were then treated with Pierce ECL Western Blotting Substrate and visualized using the Amersham ImageQuant 800 (Cytiva, Marlborough, MA).

Cryopreservation of TLOs

Matrigel embedded spheres can be frozen and thawed for future use. 2-3 weeks after passaging of spheres, CK-DCI media was removed and 1 mL of Dispase (2 mg/mL) was used to break apart the Matrigel droplet. After 30-45 minutes in normoxic incubator, the spheres were transferred to a 15 mL conical and washed with wash media to neutralize the protease, then centrifuged at 200 g for 5 minutes. Wash media was aspirated, and the pellet was incubated with 1 mL of 0.05%Trypsin/EDTA in normoxic incubator for 10-12 minutes with occasional pipetting. Once cells are in single cell suspension, they were washed again with stop media, centrifuged at 200 g for 5 minutes, and the supernatant aspirated, followed by resuspension of the pellet in a small volume of CK-DCI and counted using a hemocytometer. To freeze down, a density of 500,000 to 1 million singe cells is ideal. Cell are resuspended in equal volumes of CK-DCI media and 2x DMSO freezing medium (Quality Biological, Gaitersburg, MD) and transferred to a cryovial. Vials are immediately place in a container that allows freezing rate of -1°C/min and placed in a -80°C freezer. Next day, they are transferred to liquid nitrogen. To thaw, cryovial is places in a 37°C water bath until thawed. Cells are transferred to a 15 mL conical tube and washed with stop media, centrifuged at 200 g for 5 minutes, and aspirated. The ideal initial reseeding density post-thaw is 800 -1,600 cells per μL of undiluted Matrigel. Subsequent passages can be done at 400 cells per μL.

Single-cell cDNA library preparation and scRNA-seq

Viability of single cells was assessed using Trypan Blue staining, and debris-free suspensions of >80% viability were deemed suitable for single cell RNA Seq. Samples with lower viability were run with caution. Single-cell RNA-seq was performed on these samples using the Chromium

platform (10x Genomics, Pleasanton, CA) with the 3' gene expression (3' GEX) V3 kit, using an input of ~10,000 cells. Briefly, Gel-Bead in Emulsions (GEMs) were generated on the sample chip in the Chromium controller. Barcoded cDNA was extracted from the GEMs by Post-GEM RT-cleanup and amplified for 12 cycles. Amplified cDNA was fragmented and subjected to end-repair, poly A-tailing, adapter ligation, and 10X-specific sample indexing following the manufacturer's protocol. Libraries were quantified using Bioanalyzer (Agilent) and QuBit (Thermofisher) analysis and were sequenced in paired end mode on a NovaSeq instrument (Illumina, San Diego, CA) targeting a depth of 50,000-100,000 reads per cell.

scRNA-seq computational analysis

Sequencing data were aligned and quantified using the Cell Ranger Single-Cell Software Suite (version 6.1.2, 10x Genomics) against the provided GRCh38 (Ensembl 98) human reference genome. All further computational analysis of scRNA-seq data was performed using R version 4.1.3 (*https://www.R-project.org/.)* unless otherwise stated.

QC and processing

The aligned data was imported and processed using the R package Seurat v4.1.1[19]. Quality control for doublets and low-quality cells was achieved through exclusion of cells with less than 500 or more than 9000 transcripts and those with a higher than 20% mitochondrial gene contribution, respectively. Additionally, transcripts were retained if they counted over 0 in more than 0.5 % of all cells, otherwise excluded. Count data was then log-normalized and transcripts were scaled and centered, using built-in Seurat functions. Variable transcripts were calculated based on standardized feature values using observed mean and expected variance of a local polynomial regression model. On the resulting variable transcripts 50 principal components were computed, which in turn were used as input for uniform manifold approximation and projection

(UMAP) dimensionality reduction. For clustering analysis, a shared nearest neighbor (SNN) graph was constructed and the modularity function optimized using the Leiden algorithm.

Cell type annotation

Potential cell types present in our dataset were predicted through machine learning. In brief, a random forest classifier (SingleCellNet R package)[20] was trained on fully annotated published data by Murthy et al. and Haberman et al. and assessed on a withheld subset. This classifier was then applied to the current dataset and a matching cell type was predicted for each cell.

RNA velocity

RNA velocity was calculated in python using the packages Velocyto and scVelo, according to the developer's manual[21,22] Briefly, '.loom' files containing both exon and intron information were created from aligned raw data using Velocyto. scVelo was then used to normalize the data and compute moments. Subsequently, RNA velocity was estimated and projected onto Seurat-derived UMAP coordinates. The length and coherence of the velocity vectors, which indicate differentiation speed and directional confidence, respectively, were calculated. Finally, a dynamical model was applied to analyze transcriptional states and cell-internal latent time and subsequently recompute RNA velocities. The latent time, based solely on the transcriptional dynamics of a cell, was thereby determined.

References

1. Habermann, A. C. *et al.* Single-cell RNA sequencing reveals profibrotic roles of distinct epithelial and mesenchymal lineages in pulmonary fibrosis. *Sci. Adv.* **6**, eaba1972 (2020).
2. Basil, M. C. *et al.* Human distal airways contain a multipotent secretory cell that can regenerate alveoli. *Nature* **604**, 120–126 (2022).
3. Kadur Lakshminarasimha Murthy, P. *et al.* Human distal lung maps and lineage hierarchies reveal a bipotent progenitor. *Nature* **604**, 111–119 (2022).
4. Basil, M. C. *et al.* The Cellular and Physiological Basis for Lung Repair and Regeneration: Past, Present, and Future. *Cell Stem Cell* **26**, 482–502 (2020).
5. Herriges, M. & Morrisey, E. E. Lung development: orchestrating the generation and regeneration of a complex organ. *Development* **141**, 502–13 (2014).
6. Street, K. *et al.* Slingshot: cell lineage and pseudotime inference for single-cell transcriptomics. *BMC Genomics* **19**, 477 (2018).
7. Bergen, V., Lange, M., Peidli, S., Wolf, F. A. & Theis, F. J. Generalizing RNA velocity to transient cell states through dynamical modeling. *Nat. Biotechnol.* **38**, 1408–1414 (2020).
8. Yamamoto, Y. *et al.* Long-term expansion of alveolar stem cells derived from human iPS cells in organoids. *Nat. Methods* **14**, 1097–1106 (2017).
9. Jacob, A. *et al.* Derivation of self-renewing lung alveolar epithelial type II cells from human pluripotent stem cells. *Nat Protoc* **14**, 3303–3332 (2019).
10. Jacob, A. *et al.* Differentiation of Human Pluripotent Stem Cells into Functional Lung Alveolar Epithelial Cells. *Cell Stem Cell* **21**, 472-488.e10 (2017).
11. Chen, Y.-W. *et al.* A three-dimensional model of human lung development and disease from pluripotent stem cells. *Nat. Cell Biol.* **19**, 542–549 (2017).

12. Gonzalez, R. F., Allen, L., Gonzales, L., Ballard, P. L. & Dobbs, L. G. HTII-280, a biomarker specific to the apical plasma membrane of human lung alveolar type II cells. *J Histochem Cytochem* **58**, 891–901 (2010).
13. Olmeda, B., Martínez-Calle, M. & Pérez-Gil, J. Pulmonary surfactant metabolism in the alveolar airspace: Biogenesis, extracellular conversions, recycling. *Ann. Anat. Anat. Anz. Off. Organ Anat. Ges.* **209**, 78–92 (2017).
14. Brehier, A. & Rooney, S. A. Phosphatidylcholine synthesis and glycogen depletion in fetal mouse lung: developmental changes and the effects of dexamethasone. *Exp. Lung Res.* **2**, 273–287 (1981).
15. Chi, E. Y. The ultrastructural study of glycogen and lamellar bodies in the development of fetal monkey lung. *Exp. Lung Res.* **8**, 275–289 (1985).
16. Gotoh, S. *et al.* Generation of alveolar epithelial spheroids via isolated progenitor cells from human pluripotent stem cells. *Stem Cell Rep.* **3**, 394–403 (2014).
17. Sun, X. *et al.* A census of the lung: CellCards from LungMAP. *Dev. Cell* **57**, 112-145.e2 (2022).
18. Adams, T. S. *et al.* Single-cell RNA-seq reveals ectopic and aberrant lung-resident cell populations in idiopathic pulmonary fibrosis. *Sci. Adv.* **6**, eaba1983 (2020).
19. Butler, A., Hoffman, P., Smibert, P., Papalexi, E. & Satija, R. Integrating single-cell transcriptomic data across different conditions, technologies, and species. *Nat. Biotechnol.* **36**, 411–420 (2018).
20. Tan, Y. & Cahan, P. SingleCellNet: A Computational Tool to Classify Single Cell RNA-Seq Data Across Platforms and Across Species. *Cell Syst.* **9**, 207-213.e2 (2019).
21. Bergen, V., Lange, M., Peidli, S., Wolf, F. A. & Theis, F. J. Generalizing RNA velocity to transient cell states through dynamical modeling. *Nat. Biotechnol.* **38**, 1408–1414 (2020).
22. La Manno, G. *et al.* RNA velocity of single cells. *Nature* **560**, 494–498 (2018).

Figure legends

Figure 1. Generation and analysis of TLOs. a. Representative bright field images of TLOs generated from RUES2 ESCs. **b.** RT-qPCR analysis of TLOs between 1 and 6 passages (84 days) (n=9) compared to lung bud organoids (LBOs) at day 21 (n=3) (*$p<0.05$, student's unpaired t-test). **c.** Representative immunofluorescence images of expression of indicated markers between 1 and 6 passages after generation from RUES2 ESCs. **d.** Representative Western Blot analysis of the expression of fully processed SFPTB and SFTPC in undifferentiated RUES2 cells, in two distinct lines of TLOs derived from RUES2 ESCs, and in human adult lung. **e.** Flow cytometry for expression of HT2-280. **f.** Transmission election microscopy of TLOs. G. Representative transmission electron microscopy images (at increasing magnification from left to right) of RUES2 ESC-derived TLOs. Stars: glycogen; arrows: LBs.

Figure 2. Single cell RNAseq analysis. a. UMAP feature plots for indicated markers. **b.** Clustering analysis. **c.** Cell identity assignment based on data of Murthy et al..[3] **d.** scVelo latent time velocity analysis. **e.** Cell identity assignment based on data of Haberman et al.[1]

Figure 1

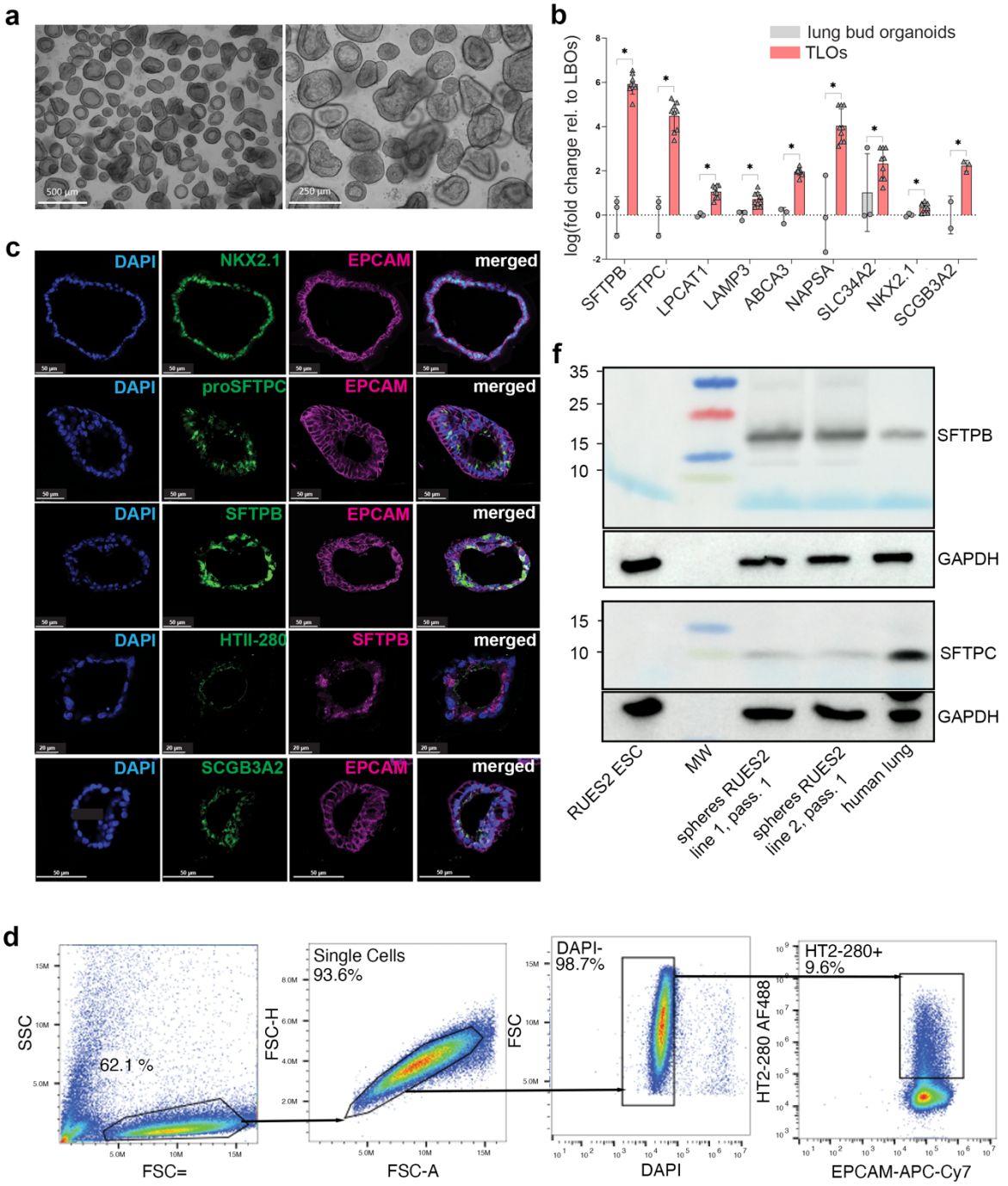
a
500 µm
250 µm
b
lung bud organoids
TLOs
log(fold change rel. to LBOs)
SFTPB
SFTPC
LPCAT1
LAMP3
ABCA3
NAPSA
SLC34A2
NKX2.1
SCGB3A2
c
DAPI
NKX2.1
EPCAM
merged
proSFTPC
SFTPB
HTII-280
SCGB3A2
f
SFTPB
GAPDH
SFTPC
RUES2 ESC
MW
spheres RUES2 line 1, pass. 1
spheres RUES2 line 2, pass. 1
human lung

d
SSC
FSC=
62.1 %
Single Cells
93.6%
FSC-H
FSC-A
DAPI-
98.7%
FSC
DAPI
HT2-280+
9.6%
HT2-280 AF488
EPCAM-APC-Cy7

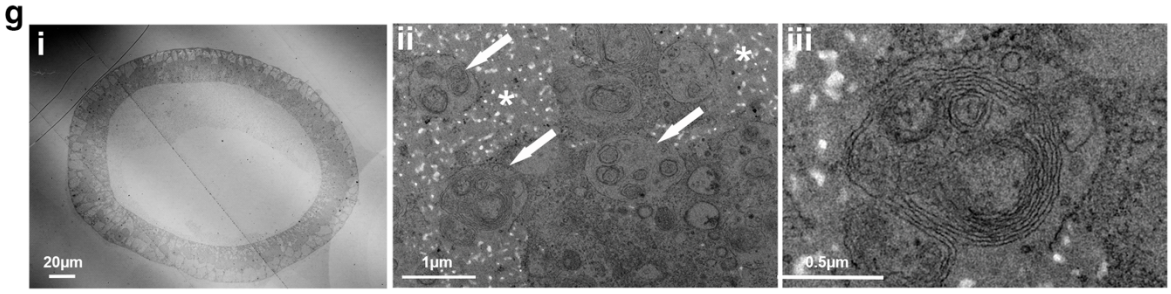
g
i
ii
iii
20µm
1µm
0.5µm

Figure 2

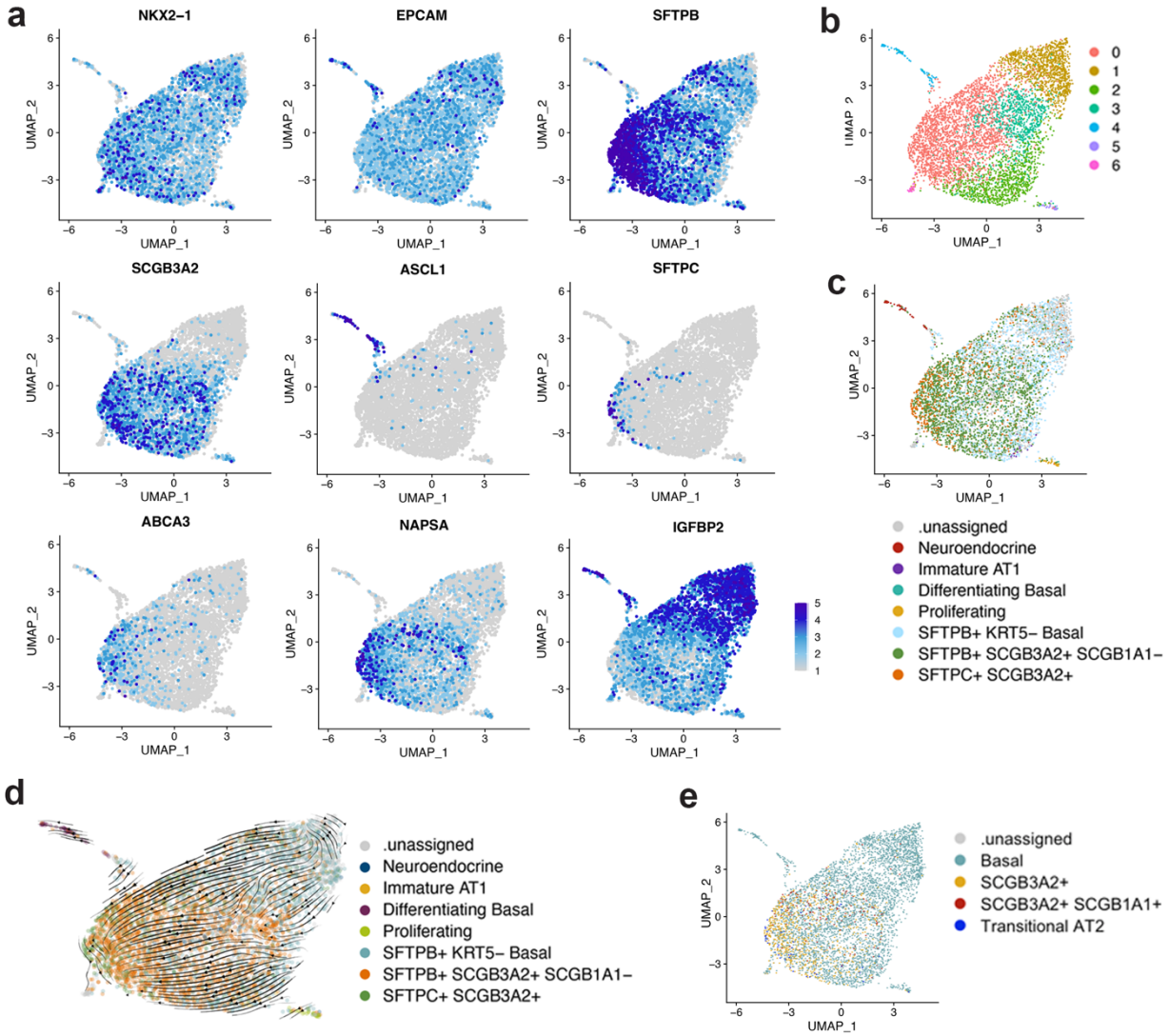
a
NKX2−1
EPCAM
SFTPB
SCGB3A2
ASCL1
SFTPC
ABCA3
NAPSA
IGFBP2
UMAP_1
UMAP_2
b
0
1
2
3
4
5
6
c
.unassigned
Neuroendocrine
Immature AT1
Differentiating Basal
Proliferating
SFTPB+ KRT5− Basal
SFTPB+ SCGB3A2+ SCGB1A1−
SFTPC+ SCGB3A2+
d
.unassigned
Neuroendocrine
Immature AT1
Differentiating Basal
Proliferating
SFTPB+ KRT5− Basal
SFTPB+ SCGB3A2+ SCGB1A1−
SFTPC+ SCGB3A2+
e
.unassigned
Basal
SCGB3A2+
SCGB3A2+ SCGB1A1+
Transitional AT2

Supplementary figures

Figure S1. a. Schematic representation of differentiation protocol (top) and representative bright field images of the various stages of the protocol (organoids: RUES2 ESCs, TLOs (right hand panels): iPSCs). **b.** TLOs generated from mixed single cells from organoids expressing either GFP or mScarlet, showing that each TLO expresses a single reporter, indicating clonality. **c.** RT-qPCR analysis of iPSC-derived TLOs (n=3) compared to lung bud organoids at day 21 (n=3, *P<0.05, students t-test). **d.** Representative immunofluorescence images of expression of indicated markers in TLOs generated from iPSCs. **e**. Lower magnification view of SCGB3A2 expression in several RUES2 ESC-derived TLOs.

Fig. S2. a. Representative Western Blot analysis of the expression of SFPTB and SFTPC, in two distinct lines of TLOs generated from RUES2 ESCs and one TLO line generated from iPSCs, and in human adult lung. **b.** Staining of ESC-derived TLOs with Lysotracker Red. **c.** Transmission election microscopy of RUES ESC-derived TLOs. Stars: glycogen; arrows: LBs.

Fig. S3. Effect of cryopreservation and of CHIR withdrawal. a. Expression of AT2 markers before and after cryopreservation of ESC-derived TLOs (n=3). **b.** Schematic representation of protocol (top) and bright field images of TLOs in CK-DCI and 5 days after withdrawal of CHIR (K-DCI). **c.** Expression of Ki67 and **d.** of cCASP3 in TLOs in CK-DCI and 5 days after withdrawal of CHIR. **e.** RT-PCR of select lung and midgut markers 1 to 5 days after withdrawal of CHIR (n=3).

Fig. S4. Heatmap of top differentially expressed genes in each cluster identified in scRNAseq of ESC-derived TLOs.

Figure S1

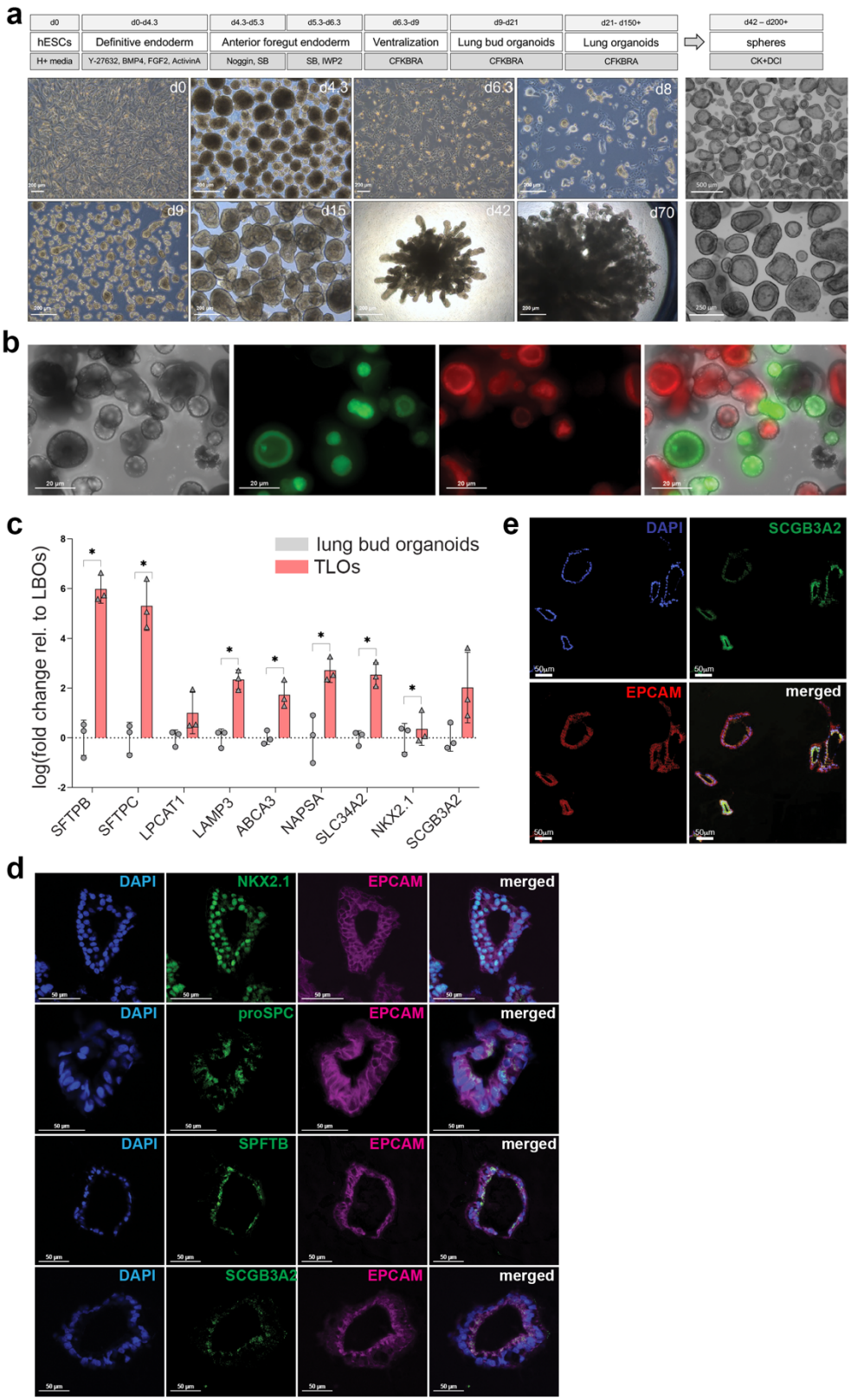
a
d0
d0-d4.3
d4.3-d5.3
d5.3-d6.3
d6.3-d9
d9-d21
d21- d150+
d42 – d200+
hESCs
Definitive endoderm
Anterior foregut endoderm
Ventralization
Lung bud organoids
Lung organoids
spheres
H+ media
Y-27632, BMP4, FGF2, ActivinA
Noggin, SB
SB, IWP2
CFKBRA
CFKBRA
CFKBRA
CK+DCI
d0
d4.3
d6.3
d8
d9
d15
d42
d70
b
c
lung bud organoids
TLOs
log(fold change rel. to LBOs)
SFTPB
SFTPC
LPCAT1
LAMP3
ABCA3
NAPSA
SLC34A2
NKX2.1
SCGB3A2
e
DAPI
SCGB3A2
EPCAM
merged
d
DAPI
NKX2.1
EPCAM
merged
DAPI
proSPC
EPCAM
merged
DAPI
SPFTB
EPCAM
merged
DAPI
SCGB3A2
EPCAM
merged

Figure S2

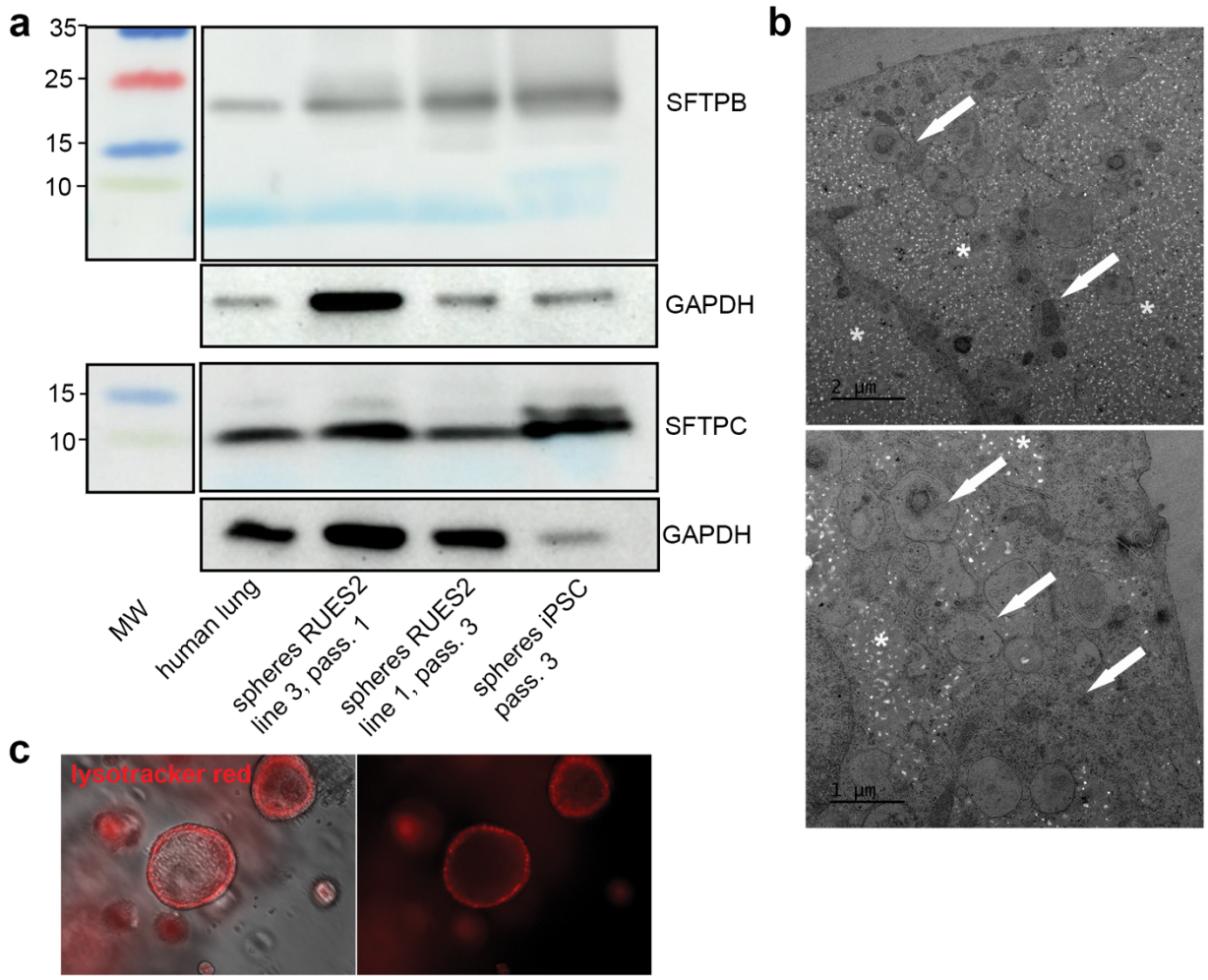
a
35
25
15
10
SFTPB
GAPDH
15
10
SFTPC
GAPDH
MW
human lung
spheres RUES2 line 3, pass. 1
spheres RUES2 line 1, pass. 3
spheres iPSC pass. 3
b
2 µm
1 µm
c
lysotracker red

Figure S3

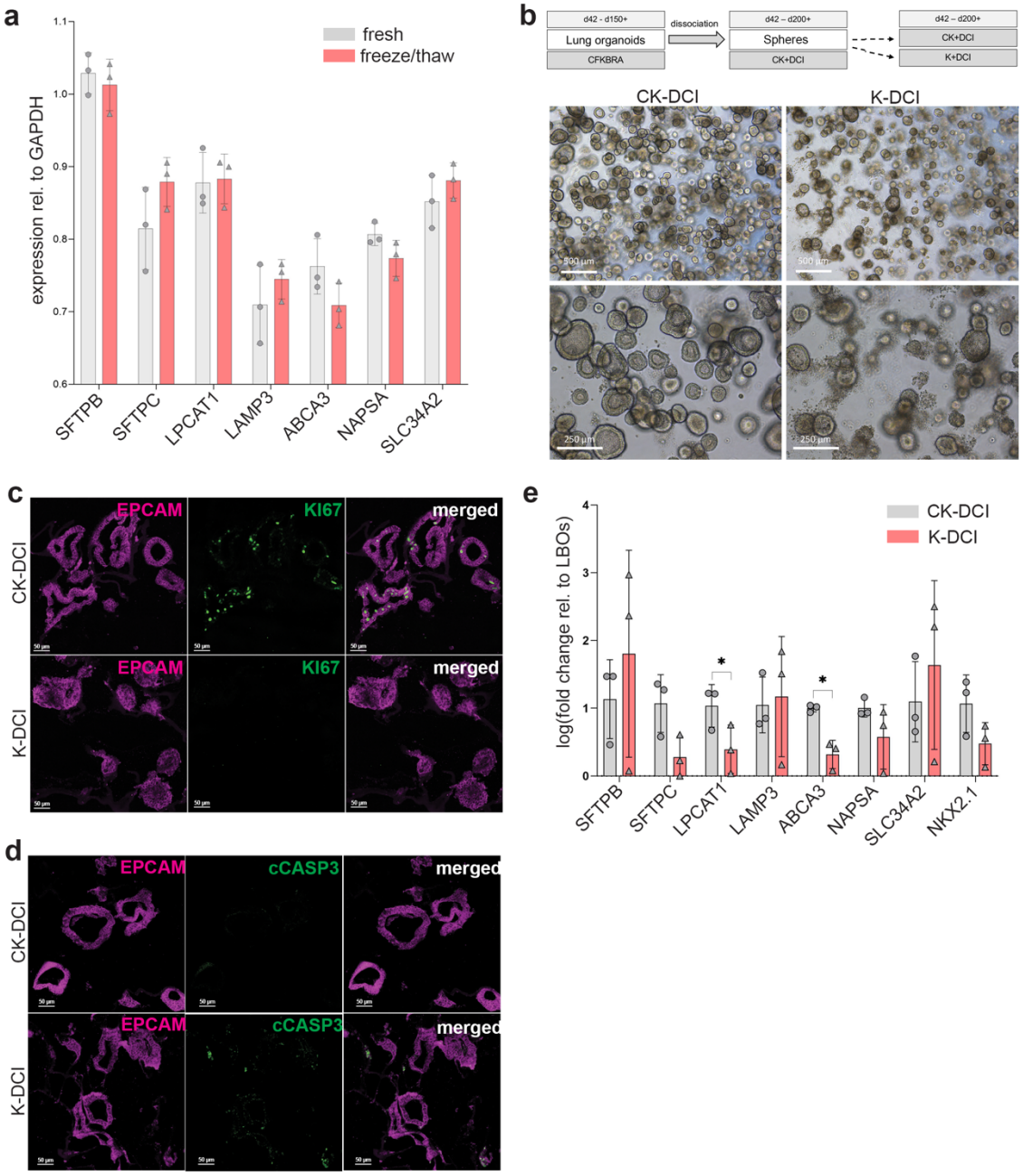
a
fresh
freeze/thaw
expression rel. to GAPDH
1.1
1.0
0.9
0.8
0.7
0.6
SFTPB
SFTPC
LPCAT1
LAMP3
ABCA3
NAPSA
SLC34A2
b
d42 - d150+
Lung organoids
CFKBRA
dissociation
d42 – d200+
Spheres
CK+DCI
d42 – d200+
CK+DCI
K+DCI
CK-DCI
K-DCI
500 µm
250 µm
c
EPCAM
KI67
merged
CK-DCI
K-DCI
50 µm
d
EPCAM
cCASP3
merged
CK-DCI
K-DCI
50 µm
e
CK-DCI
K-DCI
log(fold change rel. to LBOs)
4
3
2
1
0
*
*
SFTPB
SFTPC
LPCAT1
LAMP3
ABCA3
NAPSA
SLC34A2
NKX2.1

Figure S4

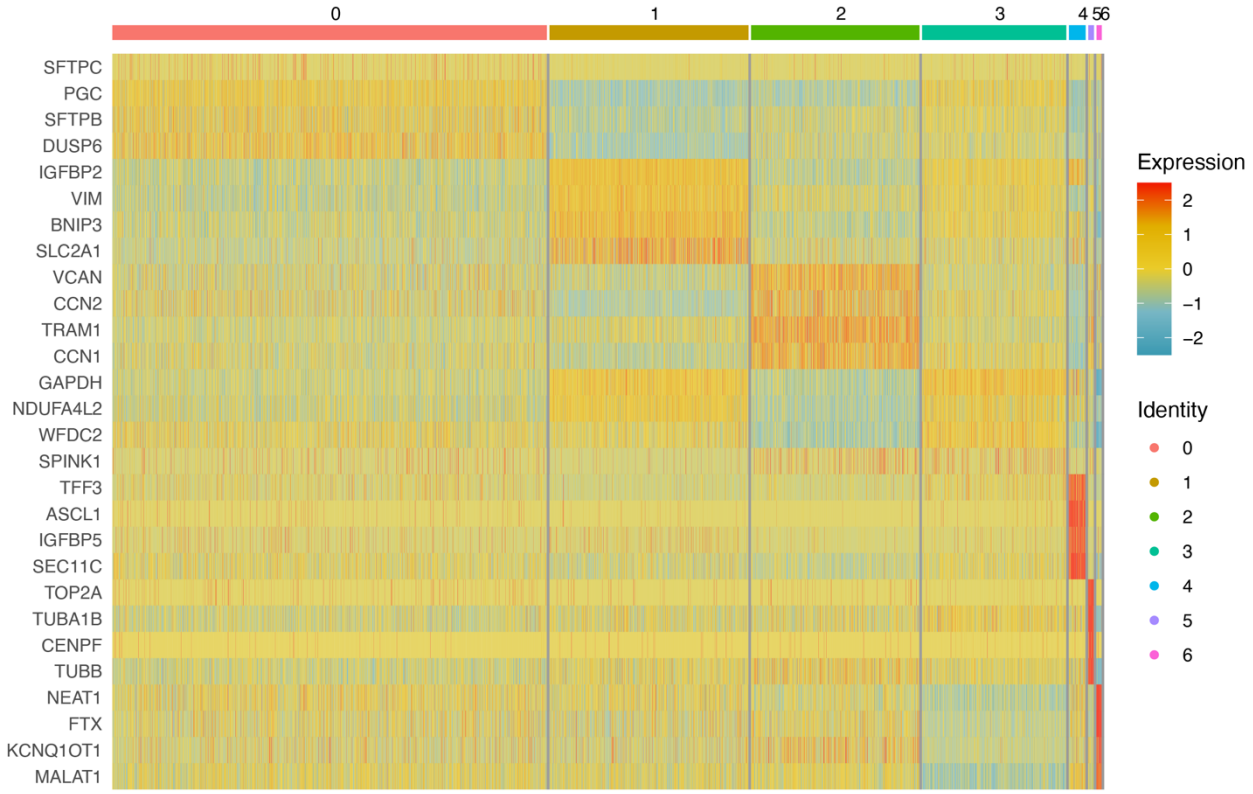
0
1
2
3
4 5 6
SFTPC
PGC
SFTPB
DUSP6
IGFBP2
VIM
BNIP3
SLC2A1
VCAN
CCN2
TRAM1
CCN1
GAPDH
NDUFA4L2
WFDC2
SPINK1
TFF3
ASCL1
IGFBP5
SEC11C
TOP2A
TUBA1B
CENPF
TUBB
NEAT1
FTX
KCNQ1OT1
MALAT1
Expression
2
1
0
−1
−2
Identity
0
1
2
3
4
5
6

Table S1: PCR primers

Gene	Forward primer	Reverse primer
ABCA3	CAGGCTGAGGGACAGGAG	TCCACAGAAGCCCTGAAGAT
GAPDH	AACTTTGGCATTGTGGAAGG	ACACATTGGGGGTAGGAACA
LPCAT1	GCCCTGTCTGTCGTCTGC	TCTTGCGCTCCGTACATCT
LAMP3	TGCTCATTTTTATGGGATTGC	TGAGTTTATTTGATGCCTTCATCTT
NAPSA	GTAGATGGAATCCTGAGCGAG	AGACAGAATGGGAAAACCGAG
NKX2.1	AGCACACGACTCCGTTCTC	GCCCACTTTCTTGTAGCTTTCC
SCGB3A2	ACTCTGGGCATTTCTGTTGAG	CATCCACCTCCGCTCTTTATC
SFTPB	GAGCCGATGACCTATGCCAAG	AGCAGCTTCAAGGGGAGGA
SFTPC	GCAAAGAGGTCCTGATGGAG	ATCACCACGACGATGAGGA
SLC34A2	CACCATCTTGCTCATACTCTCC	GTCAACCATGCAAAGGGAAAG

Table S2: Antibodies

Primary antibodies for immunofluorescent staining						
Name	**Host species**	**Clone number**	**Manufacturer and Catalog number**	**RRID**	**URL**	**Dilution Factor**
cCASP3	Rabbit	5A1E	Cell Signaling Cat # : 9664S	RRID:AB_2070042	https://scicrunch.org/resolver/RRID:AB_2070042	1:400
EPCAM	Goat	Polyclonal	R&D Systems Cat # : AF960	RRID:AB_355745	https://scicrunch.org/resolver/RRID:AB_355745	1:400
HT2-280	Mouse	TB-27	Terrace Biotech Cat # : TB-27AHT2-280	RRID:AB_2832931	https://scicrunch.org/resolver/RRID:AB_2832931	1:100
KI-67	Rabbit	D3B5	Cell Signaling Cat # : 9129S	RRID:AB_2687446	https://scicrunch.org/resolver/RRID:AB_2687446	1:200
NKX2.1	Rabbit	Polyclonal	Seven Hills Bioreagents Cat # : WRAB-1231	RRID:AB_2832953	https://scicrunch.org/resolver/RRID:AB_2832953	1:200
proSPC	Rabbit	Polyclonal	Millipore Sigma Cat # : AB3786	RRID:AB_91588	https://scicrunch.org/resolver/RRID:AB_91588	1:200
SCGB3A2	Rabbit	Monoclonal	Abcam Cat #:ab181853 (EPR11463)	-	-	1:250
SPB	Rabbit	Polyclonal	Seven Hills Bioreagents Cat # : WRAB-48604	-	-	1:500
Secondary antibodies for immunofluorescent staining						
Name	**Host species**	**Conjugate**	**Manufacturer and Catalog number**	**RRID**	**URL**	**Dilution Factor**
anti-Goat IgG (H+L)	Donkey	AF- 488	Thermo Fisher Scientific; A32814	RRID:AB_2762838	https://scicrunch.org/resolver/RRID:AB_2762838	1:200
anti-Rabbit IgG (H+L)	Donkey	AF- 488	Thermo Fisher Scientific; A21206	RRID:AB_2535792	https://scicrunch.org/resolver/RRID:AB_2535792	1:200
anti-mouse IgM Heavy Chain	Goat	AF- 488	Thermo Fisher Scientific; A21042	RRID:AB_141357	https://scicrunch.org/resolver/RRID:AB_141357	1:200
anti-Goat IgG (H+L)	Donkey	AF- 555	Thermo Fisher Scientific; A32816	RRID:AB_2762839	https://scicrunch.org/resolver/RRID:AB_2762839	1:200
anti-Rabbit IgG (H+L)	Donkey	AF- 555	Thermo Fisher Scientific; A31572	RRID:AB_162543	https://scicrunch.org/resolver/RRID:AB_162543	1:200
anti-Goat IgG (H+L)	Donkey	AF- 647	Thermo Fisher Scientific; A21447	RRID:AB_141844	https://scicrunch.org/resolver/RRID:AB_141844	1:200
Primary antibodies for Western blot						
Name	**Host species**	**Clone number**	**Manufacturer and Catalog number**	**RRID**	**URL**	**Dilution Factor**
GAPDH (HRP Conjugate)	Rabbit	14C10	Cell Signaling Technologies; 36835	-	-	1:5000
SFTPB	Rabbit	Polyclonal	Seven Hills Bioreagents Cat # : WRAB-48604	-	-	1:1000
SFTPC	Rabbit	Polyclonal	Seven Hills Bioreagents Cat # : WRAB-76694	-	-	1:1000
Secondary antibodies for Western blot						
Name	**Host species**	**Conjugate**	**Manufacturer and Catalog number**	**RRID**	**URL**	**Dilution Factor**
Anti-Rabbit IgG (H+L)	Goat	HRP	Cell Signaling Technologies; 7074	RRID:AB_2099233	https://scicrunch.org/resolver/RRID:AB_2099233	1:5000
Conjugated antibodies for flow cytometry						
Name	**Isotype**	**Conjugate**	**Manufacturer and Catalog number**	**RRID**	**URL**	**Dilution Factor**
anti-human CD326 (Ep-CAM)	Mouse IgG2b	APC	Biolegend Cat #: 324208	RRID: AB_756081	https://scicrunch.org/resolver/AB_756081	1:100